Lab on a Chip

Miniaturisation for chemistry, biology & bioengineering

www.rsc.org/loc

Volume 7 | Number 10 | October 2007 | Pages 1221–1376

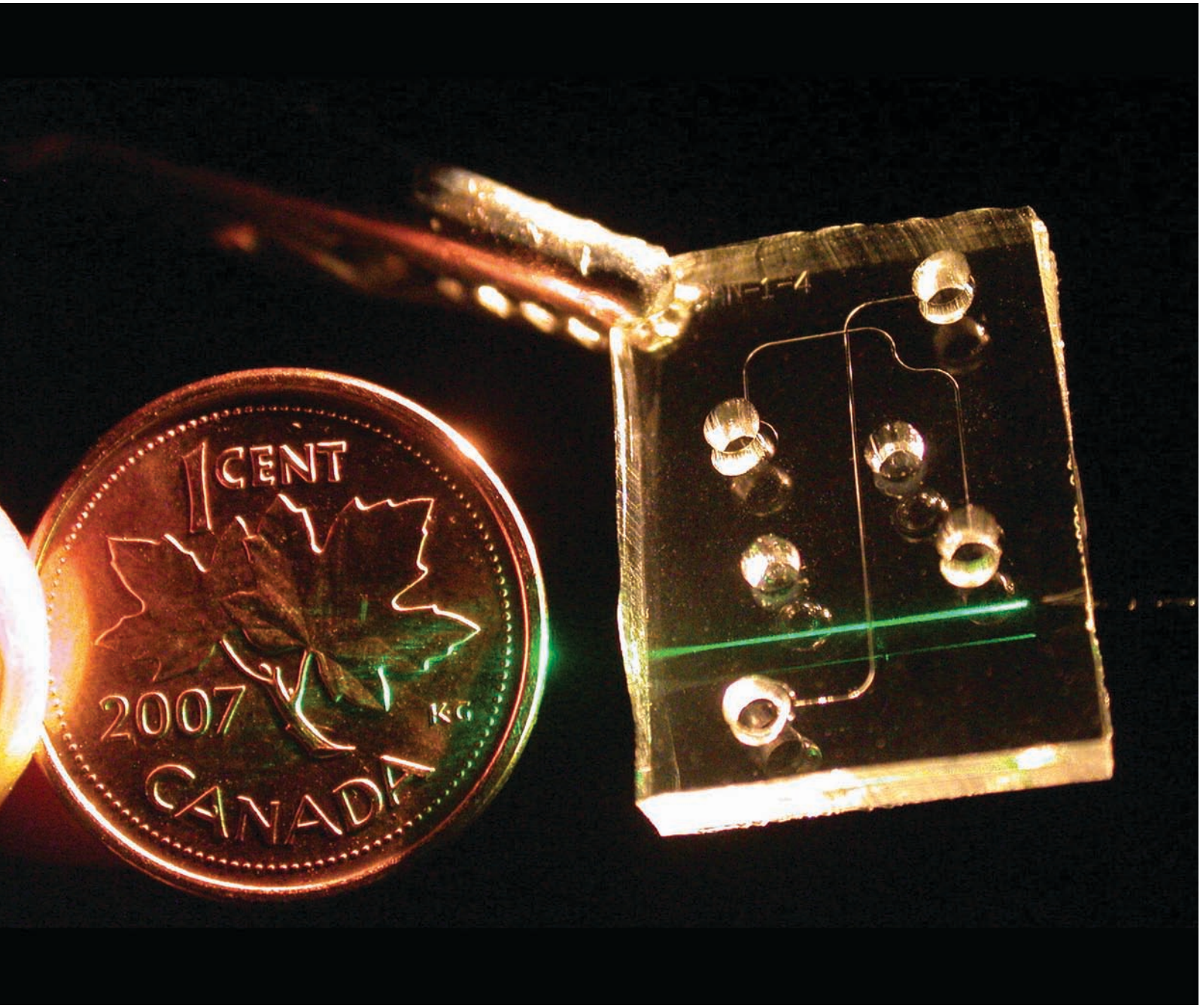

ISSN 1473-0197

RSC Publishing

Rapid fabrication of a microfluidic device with integrated optical waveguides for DNA fragment analysis

Christopher L. Bliss, James N. McMullin† and Christopher J. Backhouse†*

Received 5th June 2007, Accepted 19th July 2007
First published as an Advance Article on the web 8th August 2007
DOI: 10.1039/b708485d

The fabrication and performance of a microfluidic device with integrated liquid-core optical waveguides for laser induced fluorescence DNA fragment analysis is presented. The device was fabricated through poly(dimethylsiloxane) (PDMS) soft lithography and waveguides are formed in dedicated channels through the addition of a liquid PDMS pre-polymer of higher refractive index. Once a master has been fabricated, microfluidic chips can be produced in less than 3 h without the requirement for a cleanroom, yet this method provides an optical system that has higher performance than a conventional confocal optical assembly. Optical coupling was achieved through the insertion of optical fibers into fiber-to-waveguide couplers at the edge of the chip and the liquid–fiber interface results in low reflection and scattering losses. Waveguide propagation losses are measured to be 1.8 dB cm^{-1} (532 nm) and 1.0 dB cm^{-1} (633 nm). The chip displays an average total coupling loss of 7.6 dB due to losses at the optical fiber interfaces. In the electrophoretic separation and detection of a BK virus PCR product, the waveguide system achieves an average signal-to-noise ratio of 570 $\pm$ 30 whereas a commercial confocal benchtop electrophoresis system achieves an average SNR of 330 $\pm$ 30. To our knowledge, this is the first time that a waveguide-based system has been demonstrated to have a SNR comparable to a commercially available confocal-based system for microchip capillary electrophoresis.

1 Introduction

The development of microfluidic-based technologies for biochemical analysis has led to an increased research interest in lab-on-a-chip (LOC) systems,[1–3] which is now finding many commercial analytical and medical applications.[4,5] Advantages such as reduced sample and reagent volumes, system cost, size and power requirements, as compared to conventional systems, are key in addressing the need for point-of-care (POC) disease diagnosis. However, reduced analysis volumes lead to low signal levels since fewer molecules are present in the detection region. Though a number of detection strategies exist,[6] laser induced fluorescence (LIF) has remained the most popular in LOC systems due to the high sensitivity achievable through the use of this technique.

Confocal detection configurations are commonly used to achieve high signal-to-noise ratios (SNR) through excellent suppression of scattered light and allow for high resolution detection, making even single molecule detection possible.[7,8] However, confocal detection systems include expensive bulk optics that do not lend themselves to miniaturization—particularly an issue in the development of hand-held POC diagnostic systems. On the other hand, LOCs with integrated optical components promise a reduction in the size, cost and complexity of the system.[9] Integrated optical waveguides can be used to direct light to within microns of the sample. Also, waveguide splitters and combiners allow for a parallel architecture with multiple excitation or detection points per input or output.[10] Microscope translation stages and micro-positioners are not required since precise alignment of the optics to the detection region is achieved automatically through photolithography. Waveguides for LOC applications have been previously fabricated through oxide deposition,[11–13] ion-exchange[14,15] and anisotropic etching of silicon.[16] However, waveguide systems made of polymers such as SU-8,[17–20] UV-laser-written optical adhesives[21] and poly(dimethyl-siloxane) (PDMS)[10,22–24] have grown in popularity due to the low cost of these materials and the rapid fabrication processes based upon them.

In this paper, we describe microfluidic chips with integrated waveguides fabricated by PDMS soft lithography.[25] Waveguides are formed by filling microfluidic channels with a high refractive index liquid PDMS pre-polymer. The waveguides are used to deliver excitation light to the microchannels and to collect fluorescence from the samples under test. Optical coupling between external sources/detectors and the waveguides is achieved through optical fibers inserted into the liquid-core waveguides at the edge of the chips. The PDMS pre-polymer coats the inserted fiber, reducing reflections and scattering at the optical interface, thus increasing the coupling efficiency. Unlike previous work,[10] only a single PDMS polymer precursor is added to the waveguide channel to prevent subsequent curing that would encapsulate the interfacing optical fibers. This allows for cleaning and reuse of the chip. In addition, the design was optimized to suppress the collection of excitation (laser) light and maximize the collection of the emitted fluorescence enabling us to achieve

Department of Electrical and Computer Engineering, University of Alberta, Edmonton, Alberta, Canada. E-mail: chrisb@ualberta.ca; Fax: +1 (780) 492-1811; Tel: +1 (780) 492-2920
† These authors contributed equally to this work.

greater sensitivity, in terms of SNR, than a commercially available confocal-based system.

Numerous human diseases are detectable through genetic testing of bodily fluids. Pathogen detection in food and water is becoming more common as the availability of affordable DNA analysis technologies increases. The analysis of amplified DNA fragments is commonly used as a "fingerprinting" tool in diagnostic assays.[26] We have previously demonstrated a microfluidic-based bench-top system capable of the sensitive analysis of a BK virus (viral load) from an unprocessed urine sample using a commercial confocal detection system.[27] In the current work, we present the results of a DNA fragment analysis of a BK virus (BKV) polymerase chain reaction (PCR) product using microchip capillary electrophoresis (CE) in the miniaturized waveguide system described here. We compare these results to those obtained using a commercially available microchip-based electrophoresis system, the Microfluidic Toolkit or μTK (Micralyne, AB, Canada), using identical microchips, samples and reagents.

Detection schemes which rely on integrated optics have been successfully demonstrated for micro flow cytometry[10,28] and protein analysis[29,30] and other groups have previously used integrated optics for DNA fragment analysis. In particular, Wang *et al.* have developed a miniaturized CE system with greatly simplified optics. This system is capable of the analysis of intercalator-labeled DNA using Teflon-coated glass capillaries as waveguides with inexpensive LED excitation.[31] In an impressive demonstration of the integration achievable through LOC technology, Burns *et al.* reported the amplification, digestion, separation and detection of DNA samples on a microfluidic chip containing integrated optical filters and photosensors.[32] Though the intercalating dyes used in both of the above cases tend to be much brighter than end-labeled dyes since multiple fluorophores label a single DNA fragment, this comes at the expense of decreased separation efficiency.[33] In our work, we are able to maintain high SNRs while using end-labeled DNA. It is also desirable that the microfluidic chip in a handheld POC diagnostic system be disposable to prevent cross contamination between samples and therefore cost is an important issue. The individual microfluidic chip cost can be drastically reduced by moving the photodetector and optical interference filter off-chip, while retaining the critical optical components. Once a master has been fabricated, the material cost of each chip in our system is much less than one dollar and a set of chips can be fabricated in less than 3 h without the requirement for a cleanroom. The cost per analysis is simply the cost of an individual chip, or less if the chip were re-used, since the cost of the buffer and sieving matrix is negligible relative to the cost of the chip.

In Section 2, we describe in detail the microfluidic chip design, the fabrication procedure, the waveguide propagation and fiber-coupling properties, and compare the light-gathering efficiency of the waveguide system to a confocal system. In Section 3, a performance comparison of the waveguide system to a commercial confocal system is carried out through a separation analysis of BKV DNA fragments obtained through PCR. It is shown that the SNR of the waveguide system is higher than that of the confocal system while maintaining a comparable separation efficiency. Section 4 concludes the paper with a summary and discussion of the results.

2 Device design, fabrication and optical characterization

2.1 Design and fabrication

A schematic of the PDMS device is shown in Fig. 1. The microfluidic channels connecting the sample (S), sample waste (SW), buffer (B) and buffer waste (BW) wells are 100 × 60 μm^2 ($W \times H$), with a 19 mm injection channel (S to SW) and a 22 mm separation channel (B to BW). The liquid-core waveguides are 70 × 60 μm^2 ($W \times H$) and were designed to interface to 62.5 μm core multimode optical fibers that have a total outer diameter of 125 μm when the fiber jackets are removed. Fiber-to-waveguide couplers are fabricated by flaring out the waveguide near the edges of the chip to facilitate fiber insertion (Fig. 1). The PDMS conforms to the inserted optical fiber and the fiber core lines up well with the

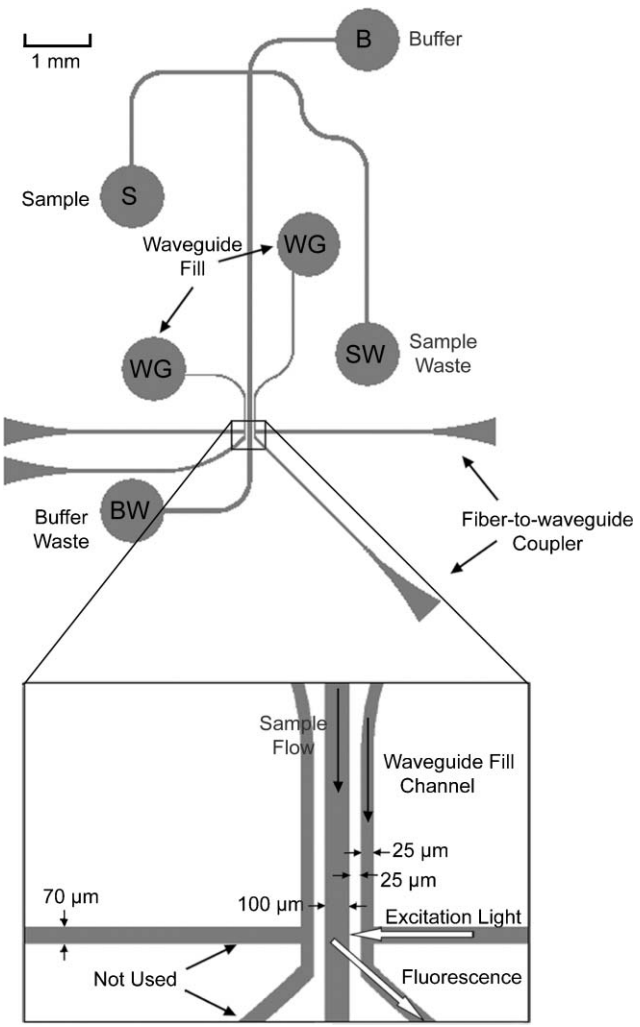

Fig. 1 A schematic of the microfluidic device with an expanded view of the detection region. The waveguides to the right of the separation channel are used for LIF, while the waveguides to the left are not used in this work.

waveguide core at the narrow end of the taper, as can be seen in Fig. 2. The fibers can be manually inserted into the coupler using a microscope with a 5× objective. Over a series of five fiber re-insertions, the average lateral misalignment was found to be less than 5 μm. The PDMS pre-polymer waveguide core coats the inserted fiber thus increasing the coupling efficiency by removing the air gap between the fiber and waveguide (Fig. 2).

The design was produced in L-Edit v3.0 (MEMS Pro 8, MEMS CAP, CA, USA) and a chrome mask was created using a pattern generator (DWL 200, Heidelberg Instruments, CA, USA). The mask was used to fabricate a master on a 10.16 × 10.16 × 0.11 cm^3 ($L \times W \times H$) borofloat substrate (Paragon Optical Company, PA, USA). A 60 μm layer of SU-8 2050 (MicroChem Corp., MA, USA) was patterned using the vendor specified protocol[34] to form the master. The master was hard baked on a contact hotplate for 1 h at 150 °C to anneal any residual cracks and to improve adhesion between the SU-8 and glass. The SU-8 master was silanized for 2 h in a desiccator under vacuum using tridecafluoro-1,1,2,2-tetrahydrooctyl-1-trichlorosilane (United Chemical Technologies, PA, USA) to prevent adhesion between the master and the PDMS.

PDMS pre-polymer and curing agent (Sylgard 184, Dow Corning, NC, USA) were mixed at a 10 : 1 (w/w) ratio. The PDMS mixture was degassed for 30 min under vacuum prior to pouring onto the master and curing at 80 °C for 2 h. A similar, featureless PDMS slab was fabricated to facilitate sealing of the microfluidic channels. The 1 mm thick PDMS slabs were removed from the mold, exposed to oxygen plasma at 100 W for 30 s and placed in contact to produce an irreversible bond. The refractive index of the cured Sylgard PDMS was verified to be 1.410 ± 0.005 at 633 nm using a Metricon Model 2010 Prism Coupler (Metricon Corp., NJ, USA). The waveguide cores were formed by adding a PDMS pre-polymer (OE-43-Part B, Gelest, PA, USA) to the waveguide channels fabricated within the bulk PDMS. The refractive index of the uncured pre-polymer was measured to be 1.429 ± 0.002 at 589 nm using a Bausch and Lomb 33–45–58 Abbe-type refractometer.

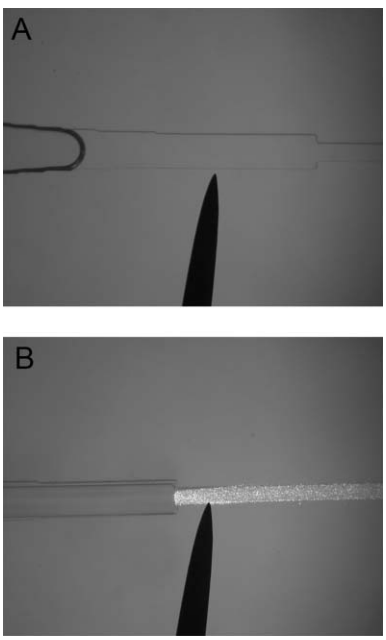

Fig. 2 Photographs from an optical microscope showing (A) an empty fiber-to-waveguide coupler partially filled with liquid and (B) scattered light observed when a live fiber is inserted into the coupler.

2.2 Waveguide characterization

Two important characteristics of optical waveguides that affect the performance of the overall system are the propagation loss per unit length and the fiber-to-waveguide coupling coefficient. Using the setup displayed in Fig. 3A, loss measurements were performed at 532 nm and at 633 nm to represent excitation and fluorescence wavelengths, respectively. The light was launched into a 3 cm long straight waveguide containing PDMS pre-polymer through an optical fiber inserted into a fiber-to-waveguide coupler. Light scattered at 90° is collected by a 1 mm plastic optical fiber at several points along the waveguide and is measured using an optical power meter (1930-C, Newport, CA, USA). Sample plots of the normalized intensity (in dB) of the scattered light are shown in Fig. 3B along with least square linear curve fits. Assuming the power of light scattered from the waveguide is proportional to the power of the confined light at each point, the propagation loss, α_{WG}, of the waveguide in dB cm^{-1} is obtained from the average slope of the plot. The measured losses were 2.9 dB cm^{-1} and 2.2 dB cm^{-1} at 532 nm and 633 nm, respectively. However, the waveguides used in the DNA fragment experiment described below were fabricated using a different SU-8 master and the propagation loss for this device was determined to be 1.8 dB cm^{-1} and 1.0 dB cm^{-1} at 532 nm and 633 nm, respectively. It is thought that the waveguide propagation loss is highly dependant on the variable quality of the SU-8 master and that the losses are primarily due to scattering by surface roughness on the waveguide walls. In future work, losses could likely be further reduced by optimizing the master fabrication process, possibly by using an edgebead removal compatible photoresist spinner or an I-line bandpass filter to improve the photolithography resolution.

The total fiber-to-waveguide coupling loss was determined by coupling a known amount of optical power from a fiber into a 1 cm long waveguide and measuring the output power from a similar fiber inserted into the taper at the opposite end. By subtracting the expected propagation loss of the 1 cm waveguide (1.0 dB at 633 nm), the total coupling loss was found. The total coupling loss includes both the fiber-to-waveguide and waveguide-to-fiber coupling losses. After a series of 8 measurements with 62.5 μm core excitation and detection fibers, where both fibers were removed, cleaned and reinserted after each measurement, the total coupling loss (L_{coup}) was found to increase from 7.3 dB to 8.4 dB with an average value of 7.6 dB. The increase in coupling loss is attributed to minor damage to the PDMS couplers due to multiple fiber re-insertions. A reduction in the fiber-to-waveguide coupling loss was observed when the detection fiber was switched to a larger 100 μm core optical fiber

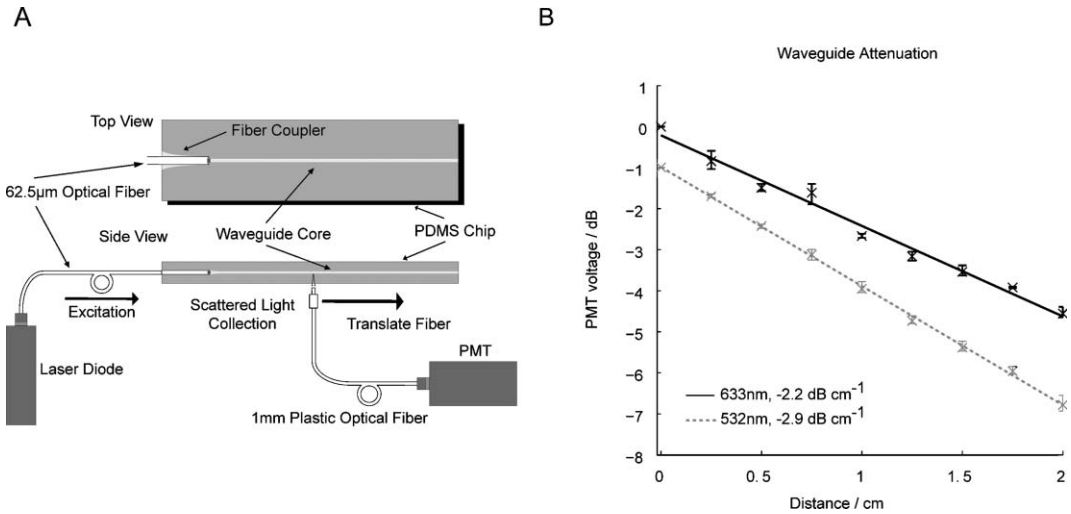

Fig. 3 (A) Experimental setup for performing waveguide loss measurements. (B) Plots of the normalized intensity along the PDMS waveguide demonstrating the propagation loss at 532 nm and 633 nm. The average waveguide attenuation is determined from a linear fit to the raw data. For clarity, the data points at 532 nm are shifted down by −1.0 dB. The primary source of uncertainty in the propagation loss measurements is drift in the laser diode intensity.

(L_{coup} = 4.8 ± 0.5 dB). However, the 100 μm core fiber was coated with a polyimide buffer, requiring removal with a flame prior to insertion into the microfluidic chip. For this reason, the 62.5 μm core fiber was found to be more convenient to use in our system and was used for the remainder of the experiments. By choosing to use the 62.5 μm core fiber, the coupling loss is increased by 7.6 − 4.8 = 2.8 dB. As described near the end of this section, we estimate that this would result in a decrease in the SNR by a factor of $10^{(2.8/20)}$ = 1.38. We felt this was a minimal change given the comparative ease of use of the polyimide-free fiber. The total optical loss through the system is given by $L_{total} = L_{coup} + \alpha_{WG} \times$ (total waveguide length in cm). For the waveguides used in the DNA fragment experiment described below, the total optical loss is 8.6 ± 0.5 dB at 633 nm.

The strength of the acquired fluorescence signal and noise due to collection of excitation light are both factors which determine the overall sensitivity of the system. The light collection efficiency (LCE) is defined as the fraction of the isotropic fluorescence emission collected and is given by $\Omega/4\pi$ where Ω is the solid angle subtended by the collection optics. An estimate of the LCE can be obtained by assuming the entire fluorescence emission originates from a point source in the center of the excitation region. For a microscope (Fig. 4A), the fraction of the isotropic emission collected by the objective lens, including all refractions at the interfaces between the sample medium and the lens, is given by[35]

$$\mathrm{LCE} = \frac{\Omega}{4\pi} = \frac{1}{2}(1 - \cos\theta_{max}) \quad (1)$$

where θ_{max} is the half-angle of the maximum cone of light collected by the lens. When the microscope is collecting light from a sample medium of index n_s, θ_{max} is related to the numerical aperture of the lens by[36]

$$\mathrm{NA} = n_s \sin\theta_{max} \quad (2)$$

In this work, the commercial confocal system used has a microscope objective with a NA of 0.55 and the sample medium has a refractive index n_s = 1.33, resulting in a collection efficiency of approximately 4.5%.

For a waveguide (Fig. 4B) of width w and height h at a distance d from the point source, the approximate solid angle subtended by the end of the waveguide is $\Omega = wh/d^2$ and therefore

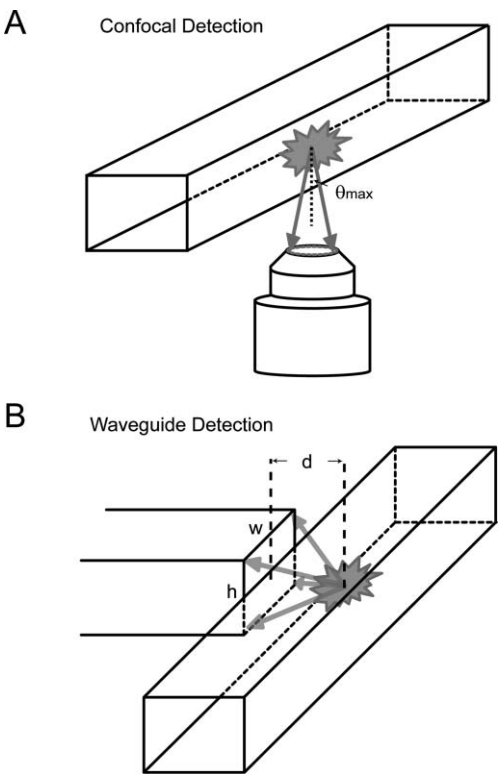

Fig. 4 A comparison of (A) confocal and (B) waveguide fluorescence collection.

$$\mathrm{LCE} = \frac{wh}{4\pi d^2} \quad (3)$$

For our waveguide system, $w \times h = 70 \times 60\ \mu m^2$, $d = 160\ \mu m$ and $n_s = 1.33$ implying a collection efficiency of approximately 1.3%. However, when d is small and Ω is large, the maximum angle of collected light is limited by the waveguide numerical aperture[36]

$$\mathrm{NA} = \sqrt{n_{\mathrm{core}}^2 - n_{\mathrm{clad}}^2} \quad (4)$$

which in our system is $\mathrm{NA} = \sqrt{(1.43^2 - 1.41^2)} = 0.24$. As above, the numerical aperture and maximum angle of light collected from a medium of index n_s are related by eqn (2). For small cone angles (as is the case here), $\sin\theta_{\max} \approx \theta_{\max}$ and the approximate solid angle is $\Omega = \pi\theta^2_{\max}$. The resulting NA-limited collection efficiency is found to be

$$\mathrm{LCE}_{\max} = \frac{\mathrm{NA}^2}{4n_s^2} \quad (5)$$

or approximately 1% in our system and is similar to the simple geometrical estimate made above. These calculations show that a small aperture waveguide placed close to the sample volume can achieve a LCE of the same magnitude as that of a confocal microscope system.

A performance indicator for the device is the SNR, which can be optimized by maximizing the LCE while limiting sources of detector noise. The benefits of an increased SNR include a lower limit of detection (LOD), typically defined as the smallest sample concentration detectable with a SNR equal to 3. The background noise in photomultiplier tube (PMT) based LIF systems is ideally shot-noise-limited and increases as the square root of the signal baseline. Careful design of the detection geometries and the use of optical filters assist in preventing scattered or reflected excitation light from reaching the detector, reducing both the signal baseline and detector shot-noise. Additionally, electrical and software low-pass filters can be used to remove high frequency shot or analog-to-digital converter (ADC) noise to increase the SNR. Additional losses in the detection optics such as vignetting and poor light collimation in confocal systems or waveguide propagation loss and fiber coupling losses in waveguide-based systems will reduce the amount of light reaching the sensor. These losses will have equal effects on the amount of fluorescence and excitation light which reach the detector and will result in a decrease in the SNR by a factor of $10^{L/10}/\sqrt{(10^{L/10})} = 10^{L/20}$, where L is the optical loss in dB.

3 Application: DNA fragment analysis

The μTK is a commercially available microchip-based electrophoresis system and is used as a benchmark in comparison with our custom-built system. The μTK provides optical detection from the underside of the microfluidic chip as seen in Fig. 5A. The light emitted from the objective was measured to be approximately 1.70 ± 0.03 mW by focusing the source onto a handheld laser power meter (T54-018, Edmund Optics, NJ, USA). As part of the μTK, the PMT data is sampled using a 16-bit ADC at 200 Hz. Further system details can be found in ref. 37. In our system (Fig. 5B), an excitation waveguide delivers light to the separation channel and the fluorescence is collected by a waveguide at an angle of 45° to the excitation waveguide (Fig. 1). Light is coupled into the excitation fiber by focusing the output from a 5 mW, 532 nm green laser diode (Holograms & Lasers Int., TX, USA) into the fiber core using a 10× microscope objective. The light emitted from the free end of the optical fiber was measured to be 3.0 ± 0.1 mW using an optical power meter (1930-C, Newport, CA, USA) prior to insertion into the excitation waveguide. Fluorescence light is captured by the collection waveguide and is coupled into a second optical fiber, which delivers light to the in-line optical filter ($OD_{532\ nm} \sim 6.7$, $T_{590\ nm} \sim 81\%$, D590/55 m, Chroma, VT, USA) prior to detection at the PMT (H5784-20, Hamamatsu, Japan). Both the excitation and detection waveguides are 5 mm in length. The PMT is sampled at 48 kHz and averaged in real-time to give an equivalent sample rate of 50 Hz.

New PDMS chips were conditioned prior to use for the first time to minimize surface effects. The channels were filled with a solution of 5% linear polyacrylamide (LPA—MW 600k–1000k) (Polysciences Inc., PA, USA) and 17% Dynamic Coating (The Gel Co., CA, USA), allowed to sit for 15 min and then were rinsed with de-ionized water. For each experiment, the PDMS chip was loaded with 6% LPA as a sieving matrix for the electrophoretic separations. The wells B, SW and BW were loaded with 3 μL of 1 × TTE buffer (tris-taurine- ethylenediaminetetraacetic acid) and the sample well (S) was loaded with 2.4 μL of autoclaved water, 0.3 μL 1 × TTE and 0.3 μL BKV PCR product, which was synthesized as described elsewhere.[27] The BKV PCR product is end-labeled with VIC dye (Applied Biosystems, CA, USA) and has a fluorescence emission peak at approximately 550 nm with a tail that extends into the red. In each system, the DNA sample was injected at a field of 158 V cm^{-1} for 100 s and separated at 136 V cm^{-1} for 110 s. Subsequent injections in the same load were reduced to 10 s. Optical detection was performed at a distance of 11.5 mm from the intersection in both the μTK and the waveguide-based system.

The optical sensitivities of the waveguide system and μTK were set to 39 V nW^{-1} and 36 V nW^{-1}, respectively, by configuring the PMT gain as shown in Table 1. The gain of the PMT in each case is chosen to maximize the detected peak height without saturating the PMT or the ADC. The SNR of signals received from both PMTs vary little with gain for gains greater than 20 000, suggesting that the PMTs in both systems are shot-noise limited.[38]

The results from 3 chip loads, averaged over 3 consecutive injection/separation runs per load, are compiled in Table 2, where each new load required replacing the sieving matrix, buffer and sample in the microfluidic chip. The SNR is indicative of the overall sensitivity of the system and is determined by dividing the average peak height above the background by the standard deviation of the background signal immediately prior to the product peak. The average SNR of the waveguide and μTK systems was found to be 570 ± 30 and 330 ± 30, respectively, demonstrating that the waveguide system consistently outperformed the confocal system in terms of sensitivity. Run-to-run variations can be

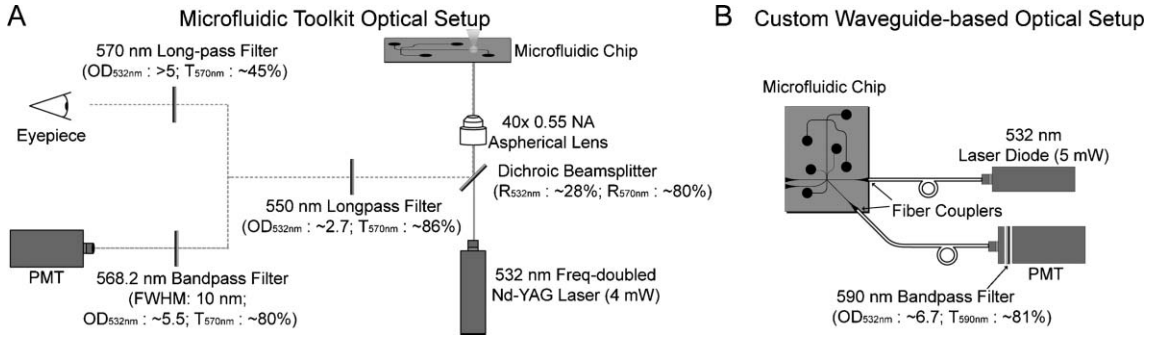

Fig. 5 A comparison of the optical setups of (A) the μTK[37] and (B) our integrated system.

Table 1 The sensitivities of the PMTs used in each system are compared at 550 nm, the emission peak for the VIC fluorescent dye. The PMT sensitivity is a product of the cathode radiant sensitivity, the gain and the effective amplifier feedback resistance. The PMT gain is tuned by setting the PMT control voltage

	Control voltage/V	Cathode radiant sensitivity @ 550 nm/A W^{-1}	Gain	Effective amplifier feedback resistance/Ω	Sensitivity @ 550 nm/V nW^{-1}
μTK PMT[a]	0.5	3.5×10^{-02}	2.0×10^{4}	5.2×10^{7}	36
Waveguide PMT[b]	0.8	7.8×10^{-02}	5.0×10^{5}	1.0×10^{6}	39

[a] H5773-01, Hamamatsu, Japan. [b] H5784-20, Hamamatsu, Japan.

attributed to slight variations in the confocal focus within the channel, fiber-to-waveguide coupling and placement of the electrodes within the wells. The position of the electrode with respect to the channel entrance can impact electrophoresis reproducibility through a non-uniform space charge distribution of ions or a change in pH[39] near the channel entrance. Since these effects are more pronounced near the electrode, close positioning of the electrode to the channel entrance has been found to decrease repeatability and increase instability in the electrophoresis currents. As explained in the following paragraph, the higher performance of the waveguide system is due to its lower level of detected excitation light even though the optical filters in the μTK provide an additional factor of 30 in terms of excitation light suppression over the waveguide system.

Results comparing typical DNA fragment separations in freshly loaded chips in each system are shown in Fig. 6. The shift in peak position is due to the slightly larger (+6 V cm^{-1}) separation field strength that was used in the waveguide system. In order to directly compare the two results, the signals have been normalized to the height of the primer peak. The SNR is calculated using the baseline noise just before the PCR product peaks that occur in the 70–80 s range. It can be seen that the μTK baseline is approximately twice that of the waveguide system and has a correspondingly higher noise assuming shot-noise-limited detection.

The baseline signal has two components—fluorescence from DNA that leaks into the separation channel and scattered excitation light. The contribution due to scattered excitation light in each system can be determined by considering the baseline during the time before any DNA reaches the detection region (prior to 40 s). The signals in this region for both systems are shown on a logarithmic scale in inset (a) of Fig. 6. Here, the waveguide system baseline is 32 dB lower than the primer peak, whereas the μTK baseline is only 16 dB lower than the primer peak indicating that the waveguide system

Table 2 Comparison of the SNR, SBR and theoretical number of plates obtained from CE runs using confocal and waveguide LIF detection systems. The noise and the baseline are calculated in the region immediately prior to the arrival of the product peak. The signal is an average of the background-corrected primer and product peak heights, where background-correcting involves subtracting the baseline from the measured peak height

		Noise: $V_{noise,std\ dev}$/V	Baseline: $V_{baseline}$/V	Signal: $V_{peak,avg}$/V	SNR: signal-to-noise ratio	SBR: signal-to-baseline ratio	Theoretical number of plates
Confocal	Load 1[a]	3.9×10^{-3}	1.0×10^{-1}	1.2	310	12	3.2×10^{4}
	Load 2[a]	3.6×10^{-3}	1.0×10^{-1}	1.1	320	11	2.0×10^{4}
	Load 3[a]	4.0×10^{-3}	1.1×10^{-1}	1.4	360	13	2.6×10^{4}
	Average	3.9×10^{-3}	1.1×10^{-1}	1.3	330	12	2.6×10^{4}
	Std dev. (% of avg)	5.3	5.6	12.5	8.6	6.1	22.5
Waveguide	Load 1[a]	1.1×10^{-2}	2.1×10^{-1}	5.7	550	26	2.0×10^{4}
	Load 2[a]	1.3×10^{-2}	2.8×10^{-1}	7.3	610	26	2.5×10^{4}
	Load 3[a]	6.5×10^{-3}	1.4×10^{-1}	3.5	560	25	1.9×10^{4}
	Average	1.0×10^{-2}	2.1×10^{-1}	5.5	570	26	2.1×10^{4}
	Std dev. (% of avg)	31.7	33.4	34.4	5.6	2.6	15.1

[a] The results for each chip load provided above are averaged over three consecutive runs.

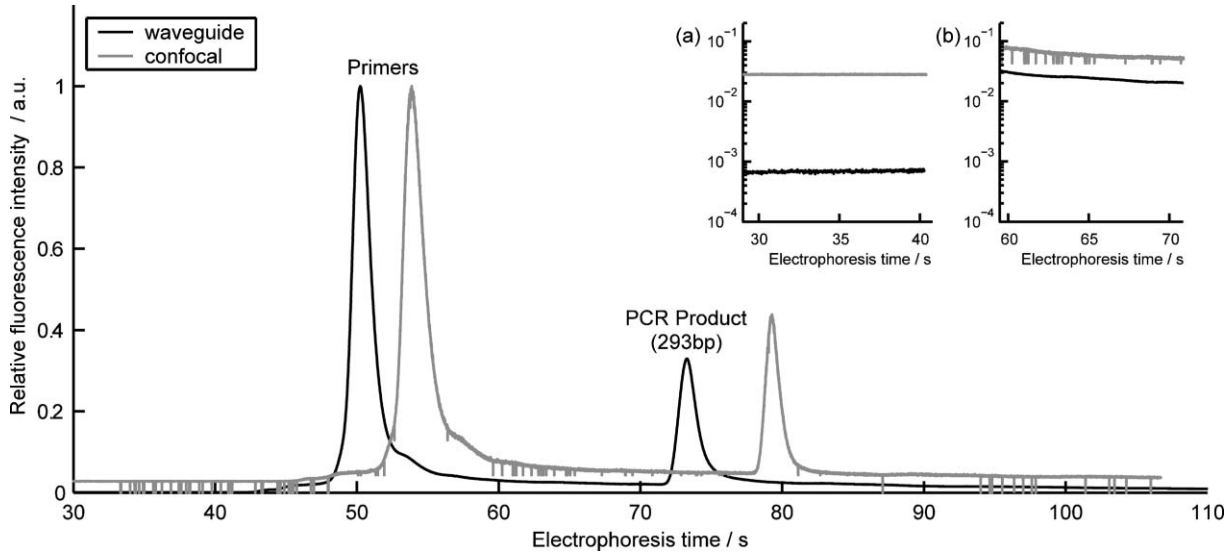

Fig. 6 An electropherogram demonstrating the detection of the BKV PCR product using the μTK and our integrated system in a freshly loaded chip. In order to directly compare the two systems, the plots have been normalized to the height of the primer peak. The shift in peak position is attributed to a 6 V cm^{-1} variation in the separation field strength between the two systems. Inset (a): An analysis of the baseline prior to the arrival of DNA highlights the contribution of excitation light to the baseline. The baseline is approximately 40 times lower for the waveguide-based system than for the μTK, suggesting improved excitation light suppression. Inset (b): An increase in the baseline on arrival of the primers is presumed to be due to DNA flow as a result of sample leakage at the injection channel. Occasional spikes in the confocal intensity data are thought to be a result of data lost due to ADC errors in the μTK system.

receives approximately 40 times less excitation light, relative to the primer peak, than the confocal system. The waveguide system has no surfaces which directly reflect excitation light into the detection waveguide whereas an estimated 3% of the excitation light in the confocal system is reflected back into the objective from the underside of microfluidic chip, assuming near-normal incident angle Fresnel reflection coefficients. After the passage of the primers, there is an increase in the signal baseline (Fig. 6, inset b) that is attributed to fluorescence emitted by DNA which enters the separation channel as a result of sample leakage (from diffusion) at the intersection between the injection and separation channels.[40] This fluorescence approximately doubles the baseline in the μTK system while accounting for almost all (97%) of the baseline in the waveguide system. In future work, further improvement in the sensitivity of the waveguide system over the μTK could be achieved by applying pull-back voltages to the sample and sample waste wells during separation to reduce DNA leakage.[40]

In addition, the low-pass filter effect of real-time data averaging during sample collection provides a factor of $M^{1/2}$ increase in the SNR, where M is the number of data points averaged.[41] In this work, we gain a factor of approximately 30 in SNR through data averaging. Since the SNR is inversely proportional to the square root of the measurement system bandwidth, similar performance gains could be expected by instead adding a bandwidth-limiting low-pass filter to the PMT output.

Due to the proprietary nature of the μTK hardware, we are unable to accurately determine the effective bandwidth of the detection electronics. While it is possible that the μTK performance could be improved through further bandwidth reduction, the fact remains that, as currently configured, the inexpensive microfabricated waveguide system outperforms the commercial confocal system.

The number of theoretical plates, N, of a separation column is a measure of the separation efficiency, and is given by[42]

$$N = 8\ln 2(t_m/W_t)^2 \quad (6)$$

where t_m is the retention time of the product and W_t is the full width at half max (FWHM) of the product peak. The average number of theoretical plates for the confocal and waveguide-based systems are $2.6 \pm 0.63 \times 10^4$ and $2.1 \pm 0.3 \times 10^4$, respectively. The slightly poorer resolution observed with the waveguide system can be attributed to the larger probe volume present within this system and the slight variation in migration time between the two systems. The tradeoff between probe volume size and resolution will be investigated in future designs.

4 Conclusions

The cost-effective integration of optical components onto microfluidic LOC devices is a precursor to the successful development of hand-held POC diagnostic systems. We have developed a miniaturized system capable of DNA fragment analysis through the use of integrated optical waveguides. We have demonstrated that waveguide detection of a viral PCR product can provide equal or greater sensitivity to that of a commercially available confocal system for LIF applications, while maintaining similar peak resolution. Though the confocal system is estimated to be able to collect a greater fraction of the fluorescence emission from the sample, the configuration of the waveguides in the miniaturized system helped to prevent excitation light from entering the collection

waveguide, providing less noise at the detector. Our custom-built miniaturized system has the potential to be integrated into a handheld system. A complete miniaturized LOC system including a fiber-pigtailed excitation laser diode, PMT, high voltage power supply, microcontroller and LCD display, can be built for less than 5% of the cost of commercially available confocal bench-top systems with comparable performance. Cost-effective mass production of the microfluidic opto-biochips through injection molding techniques is easily envisioned. Though disposable, single microfluidic chips have been reused for more than 15 electrophoretic separations involving numerous optical fiber removals and reinsertions. Future work will involve the integration of additional assays onto the LOC device and improvement and optimization of the optical detection system.

Acknowledgements

This work was supported in part by grants from the Natural Sciences and Engineering Research Council of Canada (NSERC), Canadian Institute for Photonic Innovations (CIPI), Alberta Ingenuity and the Informatics Circle of Research Excellence (iCORE). We would like to thank Viet Hoang and Jana Lauzon for assistance with the PCR products, Alex Stickel and Dammika Manage for instrumentation and protocol support and the staff at the University of Alberta Nanofab for their valuable advice.

References

1 D. R. Reyes, D. Iossifidis, P. A. Auroux and A. Manz, *Anal. Chem.*, 2002, **74**, 2623–2636.
2 P. A. Auroux, D. Iossifidis, D. R. Reyes and A. Manz, *Anal. Chem.*, 2002, **74**, 2637–2652.
3 T. Vilkner, D. Janasek and A. Manz, *Anal. Chem.*, 2004, **76**, 3373–3385.
4 C. Haber, *Lab Chip*, 2006, **6**, 1118–1121.
5 C. D. Chin, V. Linder and S. K. Sia, *Lab Chip*, 2007, **7**, 41–57.
6 K. B. Mogensen, H. Klank and J. P. Kutter, *Electrophoresis*, 2004, **25**, 3498–3512.
7 H. Craighead, *Nature*, 2006, **442**, 387–393.
8 A. J. de Mello, *Lab Chip*, 2003, **3**, 29N–34N.
9 E. Verpoorte, *Lab Chip*, 2003, **3**, 42N–52N.
10 V. Lien, K. Zhao, Y. Berdichevsky and Y. H. Lo, *IEEE J. Sel. Top. Quantum Electron.*, 2005, **11**, 827–834.
11 K. B. Mogensen, N. J. Petersen, J. Hubner and J. P. Kutter, *Electrophoresis*, 2001, **22**, 3930–3938.
12 O. Leistiko and P. F. Jensen, *J. Micromech. Microeng.*, 1998, **8**, 148–150.
13 P. Friis, K. Hoppe, O. Leistiko, K. B. Mogensen, J. Hubner and J. P. Kutter, *Appl. Opt.*, 2001, **40**, 6246–6251.
14 H. Qiao, S. Goel, A. Grundmann and J. N. McMullin, *Proc. SPIE–Int. Soc. Opt. Eng.*, 2003, **4833**, 54–59.
15 R. Mazurczyk, J. Vieillard, A. Bouchard, B. Hannes and S. Krawczyk, *Sens. Actuators, B*, 2006, **118**, 11–19.
16 D. Spicer, J. N. McMullin and H. Rourke, *J. Micromech. Microeng.*, 2006, **16**, 1674–1680.
17 K. B. Mogensen, J. El-Ali, A. Wolff and J. P. Kutter, *Appl. Opt.*, 2003, **42**, 4072–4079.
18 S. H. Huang and F. G. Tseng, *J. Micromech. Microeng.*, 2005, **15**, 2235–2242.
19 M. A. Powers, S. T. Koev, A. Schleunitz, H. M. Yi, V. Hodzic, W. E. Bentley, G. F. Payne, G. W. Rubloff and R. Ghodssi, *Lab Chip*, 2005, **5**, 583–586.
20 S. Balslev, A. M. Jorgensen, B. Bilenberg, K. B. Mogensen, D. Snakenborg, O. Geschke, J. P. Kutter and A. Kristensen, *Lab Chip*, 2006, **6**, 213–217.
21 J. N. McMullin, *Proc. SPIE–Int. Soc. Opt. Eng.*, 2000, **4087**, 1050–1055.
22 D. A. Chang-Yen, R. K. Eich and B. K. Gale, *J. Lightwave Technol.*, 2005, **23**, 2088–2093.
23 V. Lien, Y. Berdichevsky and Y. H. Lo, *IEEE Photon. Technol. Lett.*, 2004, **16**, 1525–1527.
24 O. J. A. Schueller, X. M. Zhao, G. M. Whitesides, S. P. Smith and M. Prentiss, *Adv. Mater.*, 1999, **11**, 37–41.
25 D. C. Duffy, J. C. McDonald, O. J. A. Schueller and G. M. Whitesides, *Anal. Chem.*, 1998, **70**, 4974–4984.
26 C. H. Mastrangelo, M. A. Burns and D. T. Burke, *Proc. IEEE*, 1998, **86**, 1769–1787.
27 G. V. Kaigala, R. J. Huskins, J. Preiksaitis, X. L. Pang, L. M. Pilarski and C. J. Backhouse, *Electrophoresis*, 2006, **27**, 3753–3763.
28 Z. Wang, J. El-Ali, M. Engelund, T. Gotsaed, I. R. Perch-Nielsen, K. B. Mogensen, D. Snakenborg, J. P. Kutter and A. Wolff, *Lab Chip*, 2004, **4**, 372–377.
29 S. K. Hsiung, C. H. Lin and G. B. Lee, *Electrophoresis*, 2005, **26**, 1122–1129.
30 J. Vieillard, R. Mazurczyk, C. Morin, B. Hannes, Y. Chevolot, P. L. Desbene and S. Krawczyk, *J. Chromatogr., B*, 2007, **845**, 218–225.
31 S. L. Wang, X. F. Fan, Z. R. Xu and Z. L. Fang, *Electrophoresis*, 2005, **26**, 3602–3608.
32 M. A. Burns, B. N. Johnson, S. N. Brahmasandra, K. Handique, J. R. Webster, M. Krishnan, T. S. Sammarco, P. M. Man, D. Jones, D. Heldsinger, C. H. Mastrangelo and D. T. Burke, *Science*, 1998, **282**, 484–487.
33 V. J. Sieben and C. J. Backhouse, *Electrophoresis*, 2005, **26**, 4729–4742.
34 MicroChem, 2007, SU-8 Photoresists Formulations.
35 S. L. Wu and N. J. Dovichi, *J. Chromatogr.*, 1989, **480**, 141–155.
36 E. Hecht, *Optics*, Addison Wesley, San Francisco, CA, USA, 4th edn, 2001.
37 Micralyne, 2002, Microfluidic Tool Kit Operating Manual v3.30.00, 31–38.
38 Hamamatsu, *Photomultiplier Tubes: Basics and Applications*, Hamamatsu Photonics K.K., Hamamatsu City, Japan, 3rd edn, 2006.
39 M. Macka, P. Andersson and P. R. Haddad, *Anal. Chem.*, 1998, **70**, 743–749.
40 C. S. Effenhauser, A. Paulus, A. Manz and H. M. Widmer, *Anal. Chem.*, 1994, **66**, 2949–2953.
41 R. J. Higgins, *Electronics with Digital and Analog Integrated Circuits*, Prentice Hall, Englewood Cliffs, NJ, 1983.
42 D. J. Harrison, A. Manz, Z. H. Fan, H. Ludi and H. M. Widmer, *Anal. Chem.*, 1992, **64**, 1926–1932.